16th World Congress in Computational Mechanics (WCCM)
21-26 July 2024, Vancouver, Canada
A. Korobenko, M. Laforest, S. Prudhomme, R. Vaziri (Eds)

SPACE-TIME VARIATIONAL MATERIAL MODELING: NUMERICAL SIMULATIONS FOR THE WAVE EQUATION WITH VELOCITY INITIAL AND FINAL TIME CONDITIONS

Philipp Junker[1,3], **Julian Roth**[2] **and Thomas Wick**[2,3]

[1] Leibniz University Hannover, Institute of Continuum Mechanics
An der Universität 1, 30823 Garbsen, Germany
junker@ikm.uni-hannover.de

[2] Leibniz University Hannover, Institute of Applied Mathematics
Welfengarten 1, 30167 Hannover, Germany
{roth,thomas.wick}@ifam.uni-hannover.de

[3] Cluster of Excellence PhoenixD, Leibniz University Hannover
Welfengarten 1, 30167 Hannover, Germany

Key words: Space-time, variational material modeling, wave equation, Galerkin finite element discretization

Abstract. In this work, we consider one key component, namely the wave equation, of a recently proposed space-time variational material model. The overall model is derived from a thermodynamically consistent Hamilton functional in the space-time cylinder in which mechanics, temperature and internal variables couple. Through the derivation, rather unusual end time conditions for the second-order in time wave equation arise. In order to understand their behavior better, we solely focus on the wave equation (neglecting temperature and internal variables) and formulate a Galerkin finite element discretization in time and space. Based on this discretization and the corresponding implementation, some numerical simulations are conducted. Therein, both traditional initial conditions for the displacements and the velocities are considered, as well as our newly proposed conditions for initial time and final time acting on the velocity variable only.

1 Introduction

This conference proceedings paper is devoted to a space-time Galerkin finite element discretization, the implementation and numerical simulations of the wave equation. The wave equation, to be more specific the elastic wave equation, is a component of a larger model obtained from a space-time thermodynamically consistent Hamilton functional recently considered in [14]. Therein, an extended Hamilton principle is formulated that allows to derive in a consistent fashion coupled systems for mechanics, temperature and internal variables. The same idea can be applied to flow and internal variables [13].

The main idea roots back from the classical principle of stationary action, where the action is defined as the momentum vector $m\boldsymbol{v}$ of a mass m with velocity $\boldsymbol{v}$ integrated along the path $\mathrm{d}\boldsymbol{u}$. This action transforms to

$$\mathcal{A} := \int_I 2K \, \mathrm{d}t$$

with the kinetic energy $K = \frac{1}{2}m\|\boldsymbol{v}\|^2$ and the time interval $I := (0, T)$ in which the experiment is conducted. The quantity $T > 0$ denotes the arbitrarily chosen end point in time. Replacing one of the kinetic energies by the first law of thermodynamics for conservative systems of rigid particles, i.e., $K + U = \mathrm{const}$ with the potential energy yields

$$\mathcal{A} = \int_I L \, \mathrm{d}t$$

with the Lagrange function $L := K - U$. An analogous way is possible also for deformable continua, even when dissipation takes place, see [14]. Here, it was noticed in the geometrical interpretation of a space-time cylinder, integration over the entire boundary are usually conducted, except of the top cover. Considering also the top cover yields a holistic integration over the entire surface of the space-time cylinder and has the practical implication that, instead of the common initial condition for the zeroth and first temporal derivative (displacement and velocity), conditions for the velocity at the beginning and the end of the time interval need to be prescribed.

Space-time modeling in computational mechanics and applied mathematics is well-known [15, 6, 22], but received great attention in the last three decades thanks to (parallel) computational resources in high-performance computing capacities such that, for instance, space-time multigrid solvers could be designed [9] and 4D space-time solution schemes [19]. Early work is [11, 12, 17], and work on the wave equation is [11, 12, 2, 6], and studies in fluid-structure interaction (in which the elastic wave equation is part of) include [21, 20, 8, 23].

The key objective of this paper is the computational investigation of rather unusual conditions on the wave equation. Usually, mainly due the causality in time, two initial conditions are prescribed for the second-order in time wave equation in order to have a well-posed system. These two initial conditions consist of one condition for the displacement variable and one condition for the velocity variable. In [14], starting from an extended Hamilton principle and working in the space-time cylinder, we arrived naturally into one initial condition for the velocity variable (as classically known), but also at one end time condition for the velocity variable (a new finding). First of all, the system is still assumed to be well-posed as two conditions continue to apply. However, the initial condition for the displacements is replaced by a final time condition for the velocities. This raises questions in our usual understanding as we pretend to know the end time state a priori. A closer mechanical inspection reveals that this system is not that unrealistic as we prescribe an end time condition for the velocities, which means that the system at the end time is in some thermodynamic equilibrium. For instance, $v(T) = 0$ at the end time T means that the system comes to rest, while some $v(T) = v_{end} > 0$ means that

the system moves with some constant velocity beyond the end time T. To the best of our imagination, such assumptions are valid. Finally, we notice that we do not prescribe displacement conditions, thus, the mechanical state (specifically at the end time) in terms of displacements is not known a priori, which is reasonable. We agree in view of the published literature and (justified) statements therein, e.g., [11][p. 340] that further work and understanding is necessary, for which this conference proceedings paper is one first step in terms of a numerical space-time Galerkin discretization and some numerical simulations. Therein, the main purpose is to compare classical initial conditions and the newly proposed initial/end time conditions for the velocities.

The outline of this paper is follows. In Section 2 the wave equation is introduced in space-time format and its Galerkin space-time discretization. Then, in Section 3 some numerical simulations are carried out. Our programming code is open source for which the links are provided in Section 4. Finally, our work is summarized in Section 5. Therein, future directions of our next investigations are given.

2 Space-time modeling and space-time finite element discretization

In this section, we design function spaces and we use them to state a weak formulation. In the function spaces, we work as usual: Dirichlet type conditions are built into the function spaces, while Neumann type boundary conditions appear naturally through integration by parts in the weak formulation; see e.g., [4, p.3 and Chapter 5] or [3].

2.1 Space-time domain

Let $\Omega \subset \mathbb{R}^d$ be a bounded domain (arbitrarily connected set of points), where $d = 1$ (in this paper) is the spatial dimension. Let $\partial\Omega$ be a sufficiently smooth boundary such that an outward pointing normal vector $\boldsymbol{n}$ can be defined. Next, the time interval is denoted by $I = (0, T)$ with the end time value $T \in]0, \infty[$. The closures of Ω and I are denoted by $\bar{\Omega}$ and $\bar{I}$, respectively. Now, let $\mathbb{R}^{d+1}$ be the $(d+1)$-dimensional Euclidian space with points $(\boldsymbol{x}, t)$, where $\boldsymbol{x} = (x_1, \ldots, x_d) \in \mathbb{R}^d$. The space-time cylinder is defined by

$$Q := \Omega \times I.$$

The boundary of the space-time cylinder is defined by

$$\partial Q = \{\partial\Omega \times I\} \cup \{\Omega \times \partial I\}.$$

The lateral surface (i.e., classical boundary conditions of the spatial domain) of the space-time cylinder is defined by $\{\partial\Omega \times I\}$ whereas the end faces are defined by $\{\Omega \times \partial I\}$. To capture the entire space-time cylinder, we thus need to define the boundary conditions at all surfaces. Specifically, we notice that $\partial I = \{0, T\}$ with $\partial I = \partial I_0 \cup \partial I_T$, wherein the boundary part $\partial I_0 = \{0\}$ constitutes the well-known initial condition. Specific definitions for $t = T$ (end time space-time cylinder face) are rather unusual in the classical literature, but extensively discussed and motivated in [14]. Lastly, we notice that $\partial\Omega = \partial\Omega_D \cup \partial\Omega_N$ with a Dirichlet part $\partial\Omega_D$ and a Neumann part $\partial\Omega_N$.

2.2 Function spaces

We begin with the vector-valued displacement variable $\boldsymbol{u}$. To be general, let us assume non-homogeneous Dirichlet conditions $\boldsymbol{u}^*$ on the boundary Ω_D. To this end, we define for the spatial (not yet time) components

$$V_0^u := \{\boldsymbol{u} \in H^1(\Omega) |\ \boldsymbol{u} = \boldsymbol{0} \text{ on } \partial\Omega_D\}\,,$$

where the Index 0 indicates that we are dealing with homogeneous Dirichlet boundary conditions[1]. Specifically, V_0^u serves as space for the test functions, namely the displacement variations $\delta\boldsymbol{u}$. By a suitable extension of the Dirichlet boundary data (e.g., [3, Chapter II, §2] or [16, Chapter 2]), the trial space for $\boldsymbol{u}$ is $V^u := \{\boldsymbol{u}^*|_{\Omega_D} + V_0^u\}$. In time, we assume L^2 regularity, as it is usually done [7]. This means,

$$\boldsymbol{u} \in X^u := L^2(I, V^u), \qquad \delta\boldsymbol{u} \in X_0^u := L^2(I, V_0^u)\,.$$

Again, the index 0 in X_0^u indicates that the spatial space V_0^u has homogeneous Dirichlet boundary data.

Next, we discuss the vector-valued velocity variable $\boldsymbol{v}$. Since we have no spatial boundary conditions and due to regularity, we set for the spatial part

$$V^v := L^2(\Omega)\,,$$

which is well-known in this context, e.g., [2]. The time-dependent Sobolev space then reads $X^v := L^2(I, V^v)$ such that

$$\boldsymbol{v} \in X^v, \qquad \delta\boldsymbol{v} \in X^v\,.$$

In the space-time solution, the goal is to determine both variables in a way such that [2, 10] or [24, Chapter 5] holds

$$\boldsymbol{u} \in X_0^u, \quad \boldsymbol{v} \in X^v, \quad \dot{\boldsymbol{v}} \in L^2(I, (V_0^u)^*).$$

Here, $(V_0^u)^*$ is the dual space associated to V_0^u. The dual space consists of all linear, bounded mappings from the space V_0^u into the real numbers $\mathbb{R}$, i.e., $(V_0^u)^* := L(V_0^u, \mathbb{R})$. For further information on dual spaces, we refer the reader to functional analysis textbooks, e.g., [5].

2.3 Weak and strong formulations

We denote the left hand side bilinear form by $\mathcal{A}[w](\delta w)$. Therein, w is the trial function and δw is the test function. The right-hand side is denoted by $\mathcal{L}(\delta w)$. The space-time mixed system weak formulation reads:

Proposition 1 (Weak formulation) *Let $\rho > 0$ be the density and $\boldsymbol{\sigma} = \alpha\nabla\boldsymbol{u}$ be the stress tensor, with the material parameter $\alpha = 1$. Find $\boldsymbol{v} \in X^v$ and $\boldsymbol{u} \in X^u$ such that*

$$\mathcal{A}_u[\boldsymbol{u}, \boldsymbol{v}](\delta\boldsymbol{u}, \delta\boldsymbol{v}) = \mathcal{L}_u(\delta\boldsymbol{u}, \delta\boldsymbol{v}) \quad \forall\{\delta\boldsymbol{u}, \delta\boldsymbol{v}\} \in X_0^u \times X^v$$

[1] The rigorous mathematical justification of boundary conditions requires the trace theorem; see e.g., [4, Section 1.6 and Chapter 5].

where the semi-linear form is given by

$$\mathcal{A}_u[\boldsymbol{u},\boldsymbol{v}](\delta\boldsymbol{u},\delta\boldsymbol{v}) = \int_I\int_\Omega \rho\,\dot{\boldsymbol{v}}\cdot\delta\boldsymbol{u}\,\mathrm{d}V\,\mathrm{d}t + \int_I\int_\Omega \boldsymbol{\sigma} : \nabla\delta\boldsymbol{u}\,\mathrm{d}V\,\mathrm{d}t - \int_{\partial I}\int_\Omega \rho\,\boldsymbol{v}\cdot\delta\boldsymbol{u}\,\mathrm{d}V\,\mathrm{d}s \\ - \int_I\int_\Omega \rho\,\boldsymbol{v}\cdot\delta\boldsymbol{v}\,\mathrm{d}V\,\mathrm{d}t + \int_I\int_\Omega \rho\,\dot{\boldsymbol{u}}\cdot\delta\boldsymbol{v}\,\mathrm{d}V\,\mathrm{d}t,$$

and the right-hand side functional is given by

$$\mathcal{L}_u(\delta\boldsymbol{u},\delta\boldsymbol{v}) = \int_I\int_\Omega \boldsymbol{f}^\star\cdot\delta\boldsymbol{u}\,\mathrm{d}V\,\mathrm{d}t - \int_I\int_{\partial\Omega_N} \boldsymbol{t}^\star\cdot\delta\boldsymbol{u}\,\mathrm{d}A\,\mathrm{d}t - \int_{\partial I}\int_\Omega \rho\,\boldsymbol{v}^\star\cdot\delta\boldsymbol{u}\,\mathrm{d}V\,\mathrm{d}s\,.$$

Here, $\boldsymbol{b}^\star$ are right hand side volume forces that are specified below. Traction forces are assumed to be zero, i.e., $\boldsymbol{t}^\star = 0$.

In order to make a quick relation to models that start from strong formulations, we introduce for the reader's convenience the strong form, too. When the integral formulation holds for each sub-space-time cylinder $\tilde{Q} \subset Q$ and assuming sufficient regularity of the integrands, the fundamental lemma of calculus of variations yields that the equations hold pointwise in the classical sense, and we obtain locally the equivalent mixed system in strong form: Find $\boldsymbol{u} : \bar{\Omega}\times\bar{I}\to\mathbb{R}^d$ and $\boldsymbol{v} : \bar{\Omega}\times\bar{I}\to\mathbb{R}^d$ such that

$$\begin{cases} \rho\dot{\boldsymbol{v}} - \nabla\cdot\boldsymbol{\sigma} = \boldsymbol{b}^\star & \forall(\boldsymbol{x},t)\in\Omega\times I,\\ \dot{\boldsymbol{u}} - \boldsymbol{v} = \boldsymbol{0} & \forall(\boldsymbol{x},t)\in\Omega\times I,\\ \boldsymbol{\sigma}\cdot\boldsymbol{n} = \boldsymbol{t}^\star & \forall(\boldsymbol{x},t)\in\partial\Omega_N\times I,\\ \boldsymbol{u} = \boldsymbol{u}^\star & \forall(\boldsymbol{x},t)\in\partial\Omega_D\times I,\\ \boldsymbol{v} = \boldsymbol{v}_0^\star & \forall(\boldsymbol{x},t)\in\partial\Omega\times\{0\},\\ \boldsymbol{v} = \boldsymbol{v}_T^\star & \forall(\boldsymbol{x},t)\in\partial\Omega\times\{T\}. \end{cases}$$

2.4 Galerkin finite element discretization

We employ a natural space-time finite element discretization with continuous Galerkin (cG) schemes both in space and time, i.e. time is treated as another spatial dimension in the FEM program. The discretization is based on $(d+1)$-dimensional simplices, e.g. for $d=1$ we use triangles and for $d=2$ we consider tetrahedra. In this work we consider hyperrectangular domains with $N_t\in\mathbb{N}$ elements in the temporal direction and $N_x\in\mathbb{N}$ elements in each spatial direction.

3 Numerical simulations

In this section, several computations for two configurations are carried out. The programming codes are open source and mentioned in Section 4. The space-time domain Q is composed by $\Omega=(0,1)$ and $I=(0,4)$. The right hand side is given by

$$\boldsymbol{f}^\star(\boldsymbol{x},t) = (2-\boldsymbol{x}(1-\boldsymbol{x}))\sin(t),$$

from which by inserting into the PDE, we obtain the manufactured solution

$$\boldsymbol{u}(\boldsymbol{x},t) = \sin(t)\boldsymbol{x}(1-\boldsymbol{x}), \quad \boldsymbol{v}(\boldsymbol{x},t) = \cos(t)\boldsymbol{x}(1-\boldsymbol{x}).$$

The space-time boundary conditions are obtained from the manufactured solution, specifically

$$\begin{aligned} &\boldsymbol{u}(0,t) = 0, \quad \boldsymbol{u}(1,t) = 0, \quad \boldsymbol{u}(\boldsymbol{x},0) = 0, \quad \boldsymbol{u}(\boldsymbol{x},4) = \sin(4)\boldsymbol{x}(1-\boldsymbol{x}), \\ &\boldsymbol{v}(0,t) = 0, \quad \boldsymbol{v}(1,t) = 0, \quad \boldsymbol{v}(\boldsymbol{x},0) = \boldsymbol{x}(1-\boldsymbol{x}), \quad \boldsymbol{u}(\boldsymbol{x},4) = \cos(4)\boldsymbol{x}(1-\boldsymbol{x}). \end{aligned}$$

3.1 Initial conditions for displacements and velocities

In this first example, the conditions

$$\boldsymbol{u}(\boldsymbol{x},0) = 0, \quad \boldsymbol{v}(\boldsymbol{x},0) = \boldsymbol{x}(1-\boldsymbol{x})$$

serve as initial conditions, which correspond to the classical setting. Our findings are displayed in Figure 1 in which the finite element solutions $\boldsymbol{u}_h$ and $\boldsymbol{v}_h$ are graphically compared with the manufactured solutions. Moreover, the discretization errors $\boldsymbol{u} - \boldsymbol{u}_h$ and $\boldsymbol{v} - \boldsymbol{v}_h$ are graphically displayed. In Table 1, the space-time L^2 discretization error $\|\boldsymbol{u} - \boldsymbol{u}_h\|_{L^2(\Omega\times I)}$ is evaluated. Therein, we observe quadratic convergence in the space-time error.

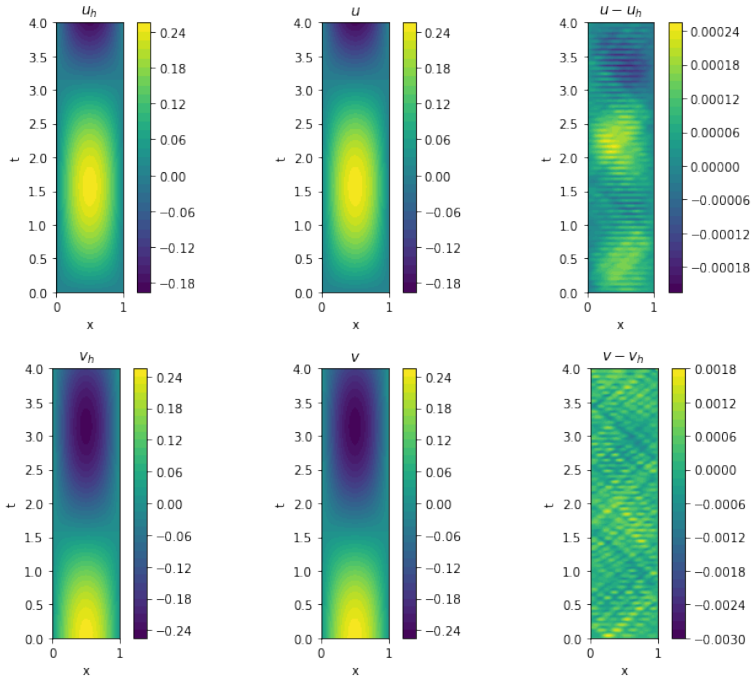

Figure 1: Example 1: Displacement and velocity field in the space-time cylinder for $N_x = 100$ and $N_t = 100$. Left finite element solutions $\boldsymbol{u}_h$ and $\boldsymbol{v}_h$. Middle analytical (reference) solutions u and v. Right graphical illustration of the discretization errors $\boldsymbol{u} - \boldsymbol{u}_h$ and $\boldsymbol{v} - \boldsymbol{v}_h$, respectively.

N_x	N_t	L^2 error
50	50	$3.7018 \cdot 10^{-3}$
100	100	$7.4361 \cdot 10^{-4}$
200	200	$2.2195 \cdot 10^{-4}$
400	400	$6.6875 \cdot 10^{-5}$

Table 1: Example 1: Space-time L^2 error $\|\boldsymbol{u} - \boldsymbol{u}_h\|_{L^2(\Omega \times I)}$.

3.2 Initial and final time conditions for velocities

In this second example, the conditions

$$\boldsymbol{v}_0^\star := \boldsymbol{v}(\boldsymbol{x}, 0) = \boldsymbol{x}(1 - \boldsymbol{x}), \quad \boldsymbol{v}_T^\star := \boldsymbol{v}(\boldsymbol{x}, T) = \cos(4)\boldsymbol{x}(1 - \boldsymbol{x})$$

serve as initial condition and final time condition, which are displayed in Figure 2. Our findings are displayed Figure 3. While the graphical solutions of $\boldsymbol{u}_h$ and $\boldsymbol{v}_h$ are similar to Figure 1, the error distributions and their nominal values are much larger; Figure 3(right). These results are confirmed by a quantitative convergence analysis made in Table 2, Table 3, and Table 4. Uniform refinement in both space and time does not yield an error reduction in the L^2 norm. The same holds for fixing the time and refining in space. Only fixing space and refining in time yield error reductions. From these computational observations, we infer that the time step size should be chosen much smaller than the spatial step size. A further analysis about the reasons remains necessary as future work. Besides the validity of the final time condition itself, also the finite element discretization itself might be a reason for the convergence behavior.

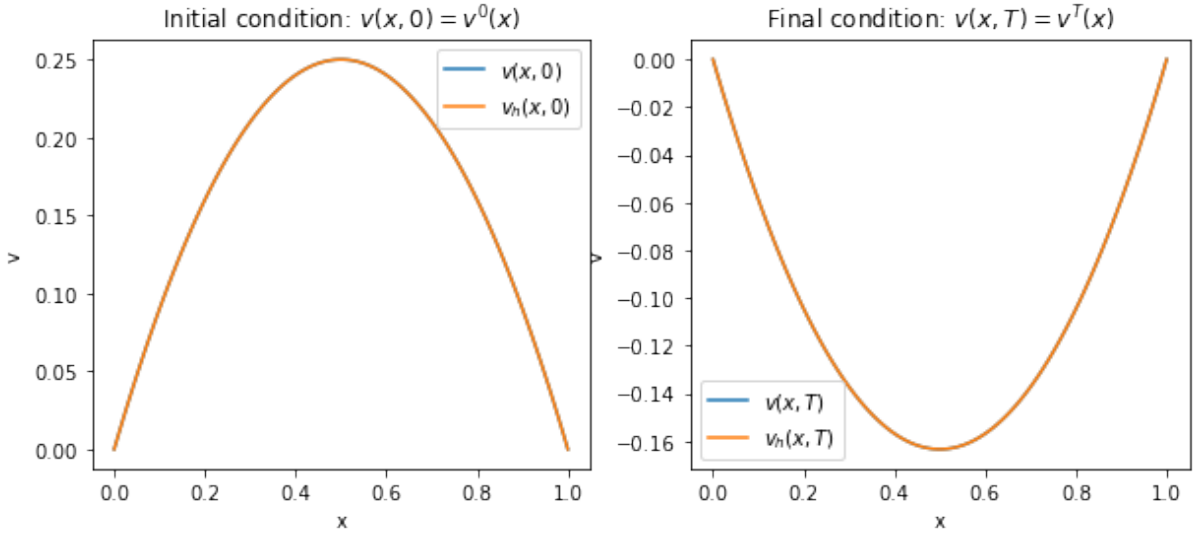

Figure 2: Example 2: Plotting the initial and final time conditions.

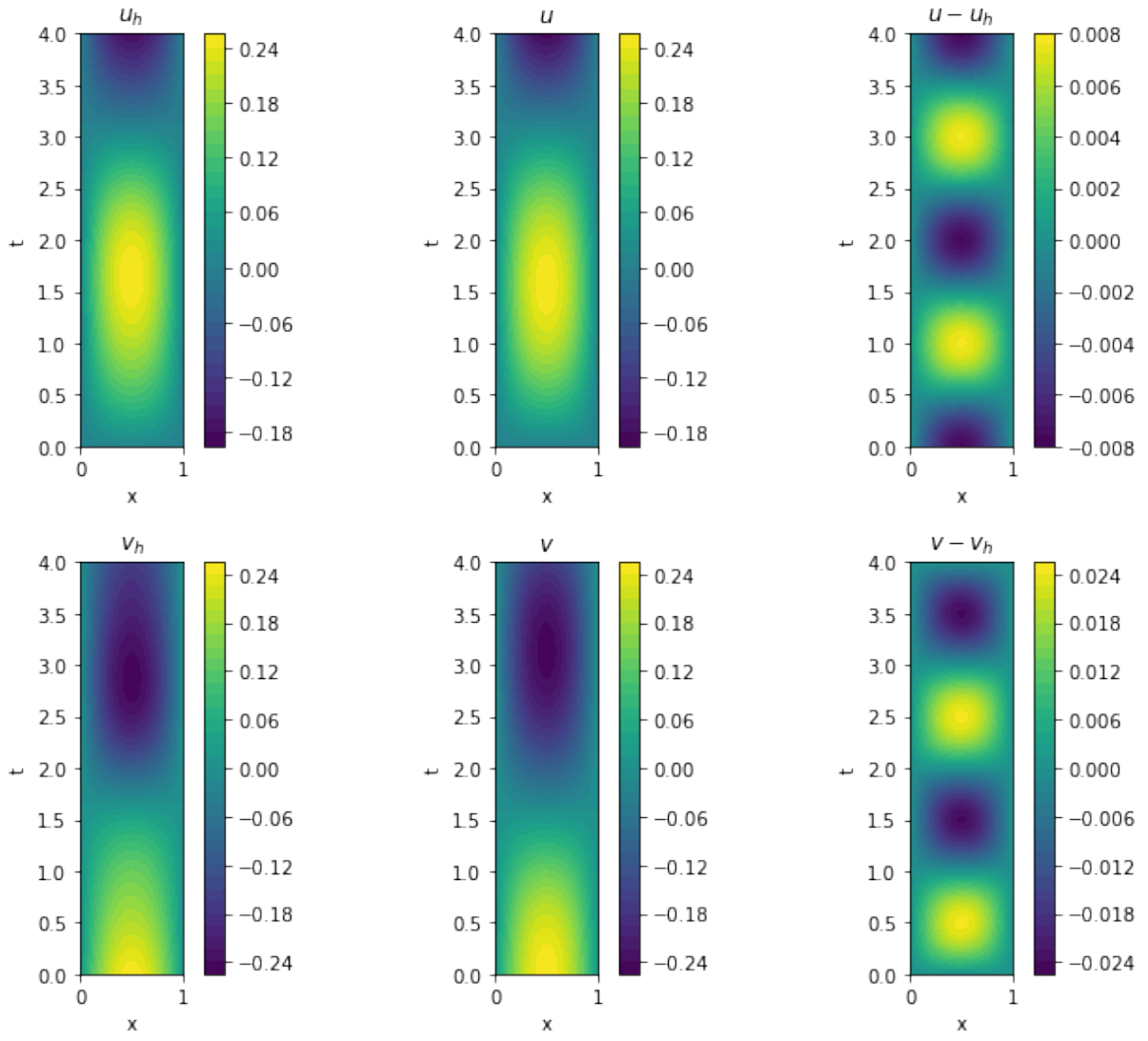

Figure 3: Example 2 (equidistant refinement): Displacement and velocity field in the space-time cylinder for $N_x = 100$ and $N_t = 1000$. Left finite element solutions $\boldsymbol{u}_h$ and $\boldsymbol{v}_h$. Middle analytical (reference) solutions $\boldsymbol{u}$ and $\boldsymbol{v}$. Right graphical illustration of the discretization errors $\boldsymbol{u} - \boldsymbol{u}_h$ and $\boldsymbol{v} - \boldsymbol{v}_h$, respectively.

N_x	N_t	L^2 error
50	50	$7.7302 \cdot 10^{-2}$
100	100	$7.7526 \cdot 10^{-2}$
200	200	$7.7180 \cdot 10^{-2}$
400	400	$7.7138 \cdot 10^{-2}$

Table 2: Example 2: Space-time L^2 error $\|\boldsymbol{u} - \boldsymbol{u}_h\|_{L^2(\Omega \times I)}$ using equidistant refinement in the time and space. The space-time error does not descrease.

N_x	N_t	L^2 error
100	50	$7.8989 \cdot 10^{-2}$
200	50	$7.9097 \cdot 10^{-2}$
400	50	$7.9198 \cdot 10^{-2}$
800	50	$7.9225 \cdot 10^{-2}$

Table 3: Example 2: Space-time L^2 error $\|\boldsymbol{u} - \boldsymbol{u}_h\|_{L^2(\Omega \times I)}$ by fixing time and refining in space only. The space-time error slightly increases.

N_x	N_t	L^2 error
50	100	$7.1580 \cdot 10^{-2}$
50	200	$5.5610 \cdot 10^{-2}$
50	400	$3.1813 \cdot 10^{-2}$
50	800	$1.5980 \cdot 10^{-2}$
50	1600	$1.0221 \cdot 10^{-2}$
50	3200	$8.6135 \cdot 10^{-3}$
50	6400	$8.1999 \cdot 10^{-3}$

Table 4: Example 2: Space-time L^2 error $\|\boldsymbol{u} - \boldsymbol{u}_h\|_{L^2(\Omega \times I)}$ by fixing space and refining in time only. The space-time error decreases with slightly less than linear convergence in the middle and later slower convergence.

4 Open source programming code

The programming code is based on FEniCS [1] and publically available on GitHub [18].

5 Conclusions

In this work, we computationally investigated the wave equation in terms of two sets of different space-time boundary conditions. First, classical initial conditions on the space-time cylinder bottom were prescribed. Second, newly proposed conditions, namely initial time and final time (space-time cylinder top cover) conditions for the velocities were prescribed. The latter derive directly from a thermodynamically consistent Hamilton functional. As these velocity-only conditions are rather unusual, the main purpose of this study was to built some further understanding on the meaning and influence of the velocity final time condition. Here, we found that that the time mesh must be finer (smaller time step sizes) than the spatial mesh. We plan to conduct further numerical studies and numerical analysis in order to understand the reasons. Furthermore, numerical realizations with space-time Galerkin finite element and computations of the full thermo-mechanics model with internal variables are planned.

Acknowledgements

This work is supported by the Deutsche Forschungsgemeinschaft (DFG) under Germany's Excellence Strategy within the cluster of Excellence PhoenixD (EXC 2122, Project ID 390833453). Moreover, we acknowledge the International Research Training Group 2657 (Deutsche Forschungsgemeinschaft (DFG) - Project ID 433082294) in which all three authors investigate modern modeling and discretization space-time methods for high-dimensional problems.

REFERENCES

[1] M. S. Alnaes, J. Blechta, J. Hake, A. Johansson, B. Kehlet, A. Logg, C. N. Richardson, J. Ring, M. E. Rognes, and G. N. Wells. The FEniCS project version 1.5. *Archive of Numerical Software*, 3, 2015.

[2] W. Bangerth, M. Geiger, and R. Rannacher. Adaptive Galerkin finite element methods for the wave equation. *Comput. Methods Appl. Math.*, 10:3–48, 2010.

[3] D. Braess. *Finite Elemente*. Springer-Verlag Berlin Heidelberg, Berlin, Heidelberg, vierte, überarbeitete und erweiterte edition, 2007.

[4] S. C. Brenner and L. R. Scott. *The mathematical theory of finite element methods*. Number 15 in Texts in applied mathematics ; 15 ; Texts in applied mathematics. Springer, New York, NY, 3. ed. edition, 2008.

[5] P. G. Ciarlet. *Linear and Nonlinear Functional Analysis with Applications*. SIAM, 2013.

[6] W. Dörfler, M. Hochbruck, J. Köhler, A. Rieder, R. Schnaubelt, and C. Wieners. *Wave Phenomena: Mathematical Analysis and Numerical Approximation*. Oberwolfach Seminars. Birkhäuser Cham, 2022.

[7] G. Duvaut and J. L. Lions. *Inequalities in Mechanics and Physics*. Springer, Berlin-Heidelberg-New York., 1976.

[8] L. Failer and T. Wick. Adaptive time-step control for nonlinear fluid-structure interaction. *Journal of Computational Physics*, 366:448 – 477, 2018.

[9] M. J. Gander and M. Neumüller. Analysis of a new space-time parallel multigrid algorithm for parabolic problems. *SIAM J. Sci. Comput.*, 38(4):A2173–A2208, 2016.

[10] C. Großmann, H.-G. Roos, and M. Stynes. *Numerical Treatment of Partial Differential Equations*. Springer, 2007.

[11] T. J. Hughes and G. M. Hulbert. Space-time finite element methods for elastodynamics: Formulations and error estimates. *Computer Methods in Applied Mechanics and Engineering*, 66(3):339 – 363, 1988.

[12] G. M. Hulbert and T. J. Hughes. Space-time finite element methods for second-order hyperbolic equations. *Computer Methods in Applied Mechanics and Engineering*, 84(3):327–348, 1990.

[13] P. Junker and T. Wick. Space-time modeling and numerical simulations of non-Newtonian fluids using internal variables. In preparation, 2024.

[14] P. Junker and T. Wick. Space-time variational material modeling: a new paradigm demonstrated for thermo-mechanically coupled wave propagation, visco-elasticity, elasto-plasticity with hardening, and gradient-enhanced damage. *Computational Mechanics*, (73):365–402, 2024.

[15] U. Langer and O. Steinbach, editors. *Space-time methods: Application to Partial Differential Equations*. volume 25 of Radon Series on Computational and Applied Mathematics, Berlin. de Gruyter, 2019.

[16] J. L. Lions and E. Magenes. *Non-Homogeneous Boundary Value Problems and Applications*. Die Grundlehren der mathematischen Wissenschaften in Einzeldarstellungen Band 181. Springer, Berlin, Heidelberg, New York, 1972.

[17] S. Mittal, A. Ratner, D. Hastreiter, and T. Tezduyar. Space-time finite element computation of incompressible flows with emphasis on flow involving oscillating cylinders. *Internat. Video J. Engrg. Res.*, 1:83–86, 1991.

[18] J. Roth. mathmerizing/SpaceTimeWave: v1.0.0. `https://doi.org/10.5281/zenodo.11352639`, 2024.

[19] A. Schafelner. *Space-time finite element methods*. PhD thesis, Johannes Kepler University Linz, 2021.

[20] K. Takizawa and T. Tezduyar. Multiscale space-time fluid-structure interaction techniques. *Computational Mechanics*, 48:247–267, 2011.

[21] T. Tezduyar, S. Sathe, R. Keedy, and K. Stein. Space-time finite element techniques for computation of fluid-structure interactions. *Comp. Meth. Appl. Mech. Engrg.*, 195:2002–2027, 2006.

[22] T. E. Tezduyar and K. Takizawa. Space-time computational flow analysis: Unconventional methods and first-ever solutions. *Computer Methods in Applied Mechanics and Engineering*, page 116137, 2023.

[23] T. Wick. Space-time methods: formulations, discretization, solution, goal-oriented error control and adaptivity. Lecture notes at Leibniz University Hannover, October 2022.

[24] J. Wloka. *Partial differential equations*. Cambridge University Press, 1987.